Search for an ELM suppression regime with non-axisymmetric magnetic perturbations at low edge collisionality in ASDEX Upgrade

W. Suttrop, L. Barrera Orte, R. Fischer, J. C. Fuchs, R. M. McDermott, A. Mlynek, T. Pütterich, S. K. Rathgeber, E. Viezzer, E. Wolfrum, and the ASDEX Upgrade Team

Max-Planck-Institut für Plasmaphysik, EURATOM Association,
D-85740 Garching, Germany

Introduction

The enhancement of ASDEX Upgrade with a new set of in-vessel saddle coils at the low-field side above and below midplane has allowed the identification of a robust scenario by which type-I ELMs give way to a distinct form of small, benign ELMs with much reduced power to the divertor [1, 2, 3, 4]. The main access condition can be described as a minimum pedestal density [5], which translates, for varying other plasma parameters, to pedestal electron collisionalities above $\nu_e^* \sim 0.8$. A remaining question is how the DIII-D low collisionality ELM suppression regime [6] can be reproduced in ASDEX Upgrade which is equipped with a fully tungsten-cladded first wall. Operationally, this implies that the tungsten impurity inward transport must be avoided in H-mode which is typically achieved by strong central wave heating and, in most cases, gas puffing.

Safety factor scan with $n = 2$ resonant magnetic perturbation

The present experiment aims to achieve the lowest possible H-mode pedestal collisionality. Figure 1 shows time traces of typical discharges with $I_p = 0.8$ MA, and ramped $B_t = 2.3 - 2.7$ T to vary the edge safety factor from $q_{95} = 4.8 - 5.8$, around optimum alignment (resonance) with an $n = 2$ magnetic perturbation (MP), to detect possibly narrow windows for ELM suppression. During the MP phase, zero gas puff is used, resulting in a pedestal collisionality around $\nu_e^* = 0.5$. The core radiated power increases slowly, indicating that the heavy impurity concentration increases in the plasma, however, accumulation and a thermal collapse are avoided for the entire programmed MP pulse length. This is achieved by using a plasma configuration with large wall clearance, reduced volume and reduced elongation (Fig. 2). A similar experiment has been performed with resonant MP at $q_{95} = 3.0$ (shot 29525) and $q_{95} = 3.5$ [2]. However, complete ELM suppression was not found in either case.

Torque input scan with resonant and non-resonant $n = 1$ perturbations

We now examine the possibility that ELM suppression is connected with the existence of a large magnetic island or stochastic field at the plasma edge that prevents expansion of the edge pressure gradient region to a point where an ELM crash is induced [7]. Generation of an island requires a resonant MP which penetrates through the H-mode edge barrier region, which, however, contains many simultaneously resonant surfaces. Two-fluid theory [8] suggests that with finite $v_{e,\perp}$ on resonant surfaces shielding currents are induced, offering the possibility to influence MP penetration in the core plasma by varying plasma rotation. However, $v_{e,\perp} = 0$ can be obtained only in the core plasma and not at the H-mode edge because of the strong diamagnetic velocity in the gradient region which in practice cannot be offset by a similarly large fluid flow. The island hypothesis is tested in low collisionality ($\nu_e^* \sim 0.5$) plasmas with

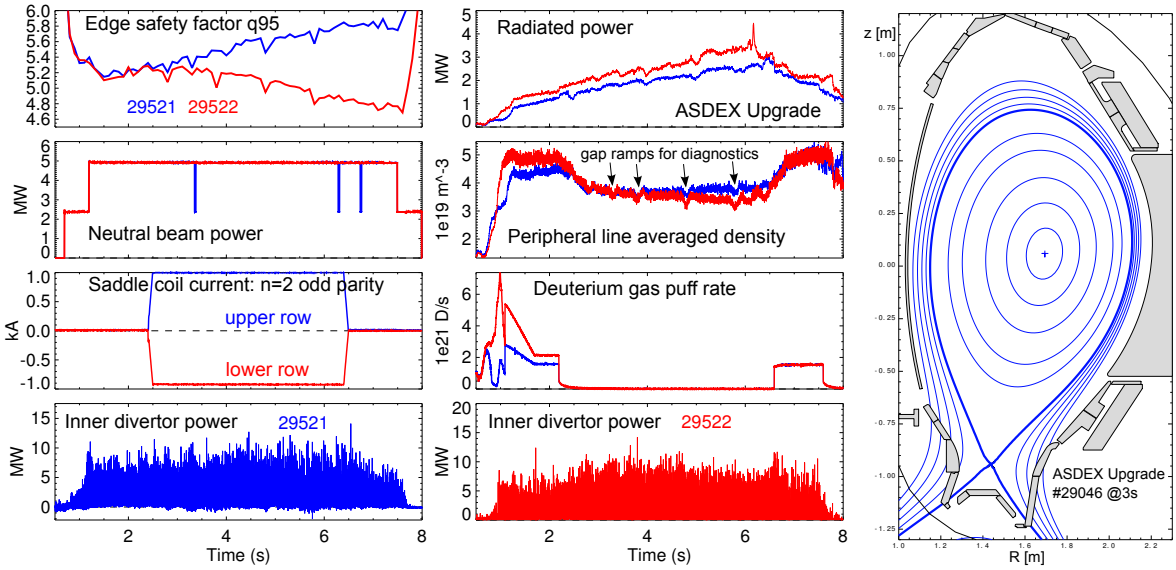

Figure 1: Time traces of H-mode plasmas with q_{95} ramps and no gas puff to detect possible ELM suppression windows.

Figure 2: Plasma shape with large wall clearance.

varying heating mix (neutral beams vs. RF heating) and hence varying momentum input to the plasma. Resonant and non-resonant $n = 1$ MP is applied as shown in Fig. 3 (a) and (b), respectively, where at the top the vacuum perturbation field normal to the $q = 2$ surface is shown vs. unfolded toroidal (Φ) and poloidal straight field line angles (θ^*) on that surface,

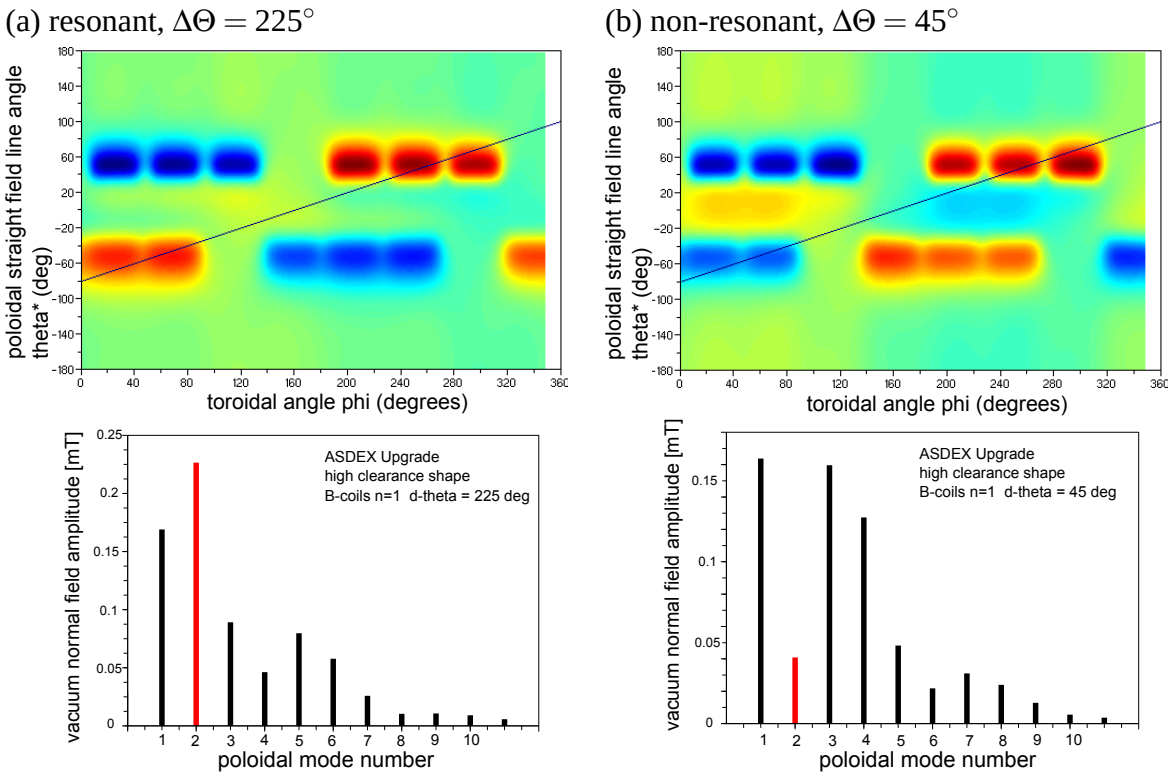

Figure 3: Perturbation field structure and poloidal mode number spectra of main toroidal harmonic, $n = 1$, for (a) resonant and (b) non-resonant configurations.

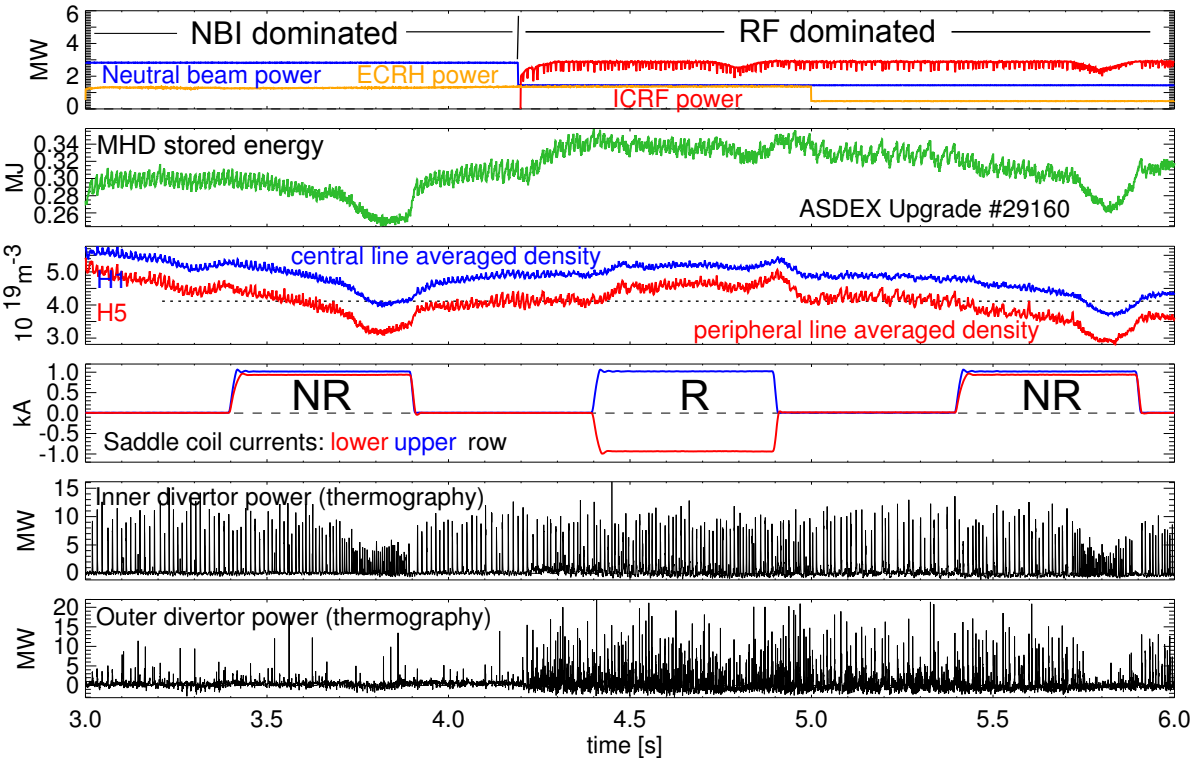

Figure 4: Variation of torque input and resonance condition of the magnetic perturbation. With a non-resonant perturbation (NR), plasma density and ELM losses are reduced.

and the poloidal mode number spectrum for the main toroidal component $n = 1$. By variation of the toroidal phase angle between the upper and lower coil rows, the vacuum resonant MP amplitude at the $q = 2$ surface ($m = 2$) is varied by a factor of 6.

Time traces of one pulse (29160) are shown in Fig. 4. Two heating phases are compared, NBI dominated ($P_{\mathrm{NBI}} = 5$ MW, $P_{\mathrm{ECRH}} = 2.4$ MW) and RF dominated ($P_{\mathrm{NBI}} = 2.5$ MW, $P_{\mathrm{ICRF}} = 5$ MW, $P_{\mathrm{ECRH}} = 0.8 - 2.4$ MW). In both cases, clear effects of a non-resonant MP (Fig. 3 b) are observed: The plasma density drops by one third, along with it the plasma stored energy, and the frequency of type-I ELMs increases by up to a factor of two, along with the reduction of stored energy drop ΔW_{ELM} and inner divertor power load by a factor of two. With optimum resonant perturbation (Fig. 3 a) the density increases slightly and no significant effect on ELMs is seen. It should be noted that the strong in-out asymmetry of divertor ELM loads with dominant beam heating disappears with dominant RF heating, except for the end of the non-resonant MP pulse.

Fig. 5 shows toroidal plasma rotation profiles, measured by charge exchange recombination spectrocopy of boron impurities, without and with non-resonant MP for different NBI/RF heating mix. Rotation braking is largest for intermediate NBI power fraction (one source, blue symbols) which also corresponds to the smallest $v_{\mathrm{e},\perp}$ in the plasma core. The effect on plasma rotation is negliglible with optimum resonance for the $q = 2$ surface. The experiment has also been repeated with coils phasing optimised for (non-) resonant MP at the $q = 5$ surface, with intermediate effect on plasma rotation.

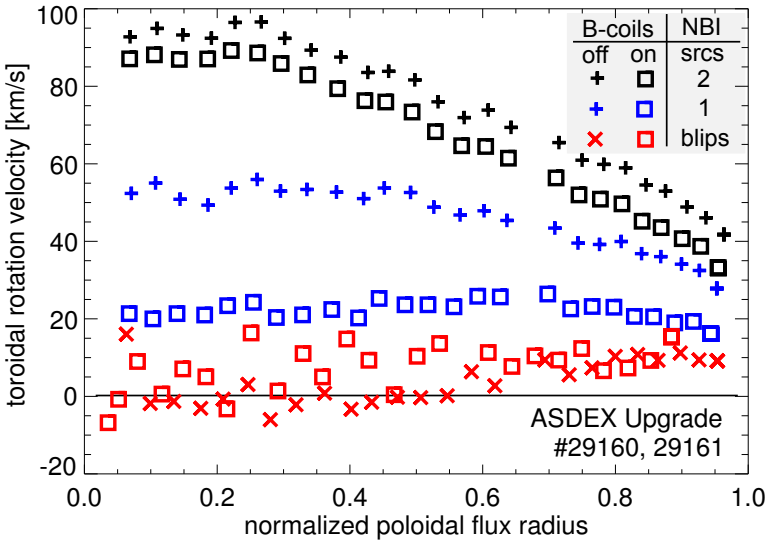

Figure 5: Toroidal plasma rotation profiles with different torque input, with B-coils on and off ($n = 1$, non-resonant configuration).

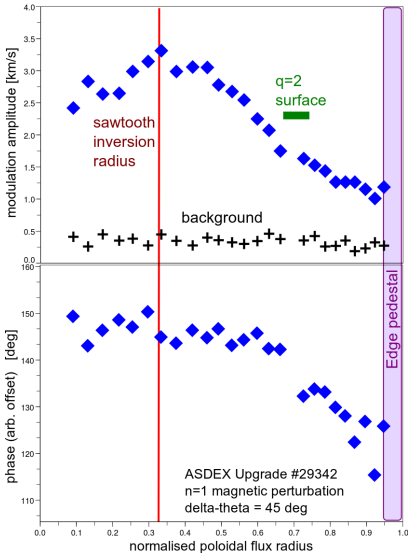

Figure 6: Amplitude and phase of toroidal rotation response to B-coil current modulation.

Conclusions and Discussion

As a surprising result, density pump-out and effects on ELMs and plasma rotation are strongest for an MP which is *non*-resonant at the $q = 2$ resonant surface, i.e. in the plasma core. This raises questions about the mechanism of the MP torque on the plasma. The torque deposition radius can be measured by modulating the MP coil current in analogy with momentum transport studies with modulated ECRH. Fig. 6 shows amplitude and phase profiles of the boron toroidal velocity with a 2 Hz modulation of the coil current. The amplitude peak shows clearly that torque is deposited at $\rho_p = 0.33$, at the $q = 1$ surface as confirmed by ECE observation of the sawtooth inversion radius. There is also a clear modulation of the $m = 1, n = 1$ sawtooth precursor mode frequency in synch with the saddle coil current, which demonstrates $J \times B$ interaction with this mode rather than an island at the $q = 2$ surface or NTV at the plasma edge as the dominant torque source. Field shielding at the $q = 2$ surface is avoided by minimising the resonant field there and shielding at outer rational surfaces ($q = 3, 4, 5$) is small because of small $v_{e,\perp}$. The question of RMP full ELM suppression at low ν^* is not solved with these experiments, as obviously a necessary requirement has not been met. In future experiments, we are planning to attempt further reduction of pedestal collisionality and finer-tuned scans around the resonance condition. However, it should be noted from Fig. 3 that the poloidal MP spectrum is broad, and only q-windows to *avoid* a resonant field are narrow.

References

[1] W Suttrop *et al*, Phys. Rev. Lett. **106** (2011) 225004
[2] W Suttrop *et al*, Plasma Phys. Control. Fus. **53** (2011) 124014
[3] S K Rathgeber *et al*, this conference, paper P4.108
[4] L Barrera *et al*, this conference, paper P4.113
[5] R Fischer *et al*, Plasma Phys. Control. Fus. **54** (2012) 115008
[6] T E Evans *et al*, Phys. Rev. Lett. **92** (2004) 235003
[7] M R Wade *et al*, IAEA FEC 2012, EX/3-1; P B Snyder *et al*, Phys. Plas. **19** (2012) 056115
[8] M Bécoulet *et al*, Nucl. Fusion **52** (2012) 054003